

Investigation of Small Scale Helicopter Servo-Actuator Performance Using Frequency Sampling Filters

Bart Gladysz Liuping Wang

*School of Electrical and Computer Engineering
RMIT University, Melbourne, Australia*

s2006892@student.rmit.edu.au liuping.wang@rmit.edu.au

Abstract: This paper addresses the performance of electric servo-actuators as part of a helicopter control linkage system. The development of a helicopter flight control system initially requires a non-linear model capable of accurately predicting the aircraft dynamics. The first step of this non-linear model represents the servo-actuator system, which transmits the pilots control inputs to the main rotor system. A series of system identification experiments were performed on a cyclic system servo-actuator under different operating conditions, and the servo-actuator step responses were estimated using a Frequency Sampling Filter. A performance comparison is made for a zero load bench test and the aircraft load condition in order to determine the most accurate representation of the servo-actuator dynamics for helicopter flight applications.

Keywords: System Identification, Parameter estimation, Frequency sampling filters, Actuators, Servo systems.

1. INTRODUCTION

Control surface deflection within conventional helicopters is achieved through hydro-mechanical actuator systems. This type of actuator is able to produce the large forces required to manipulate the orientation of a rotating main rotor disc. Smaller helicopters such as Unmanned Aerial Vehicles (UAV) and Remote Controlled (RC) models utilise electric servo-actuators due to smaller force requirements. Hydro-mechanical actuators are controlled directly by the pilots control inputs, which are amplified through the hydraulic system and transmitted to the control surfaces of the aircraft to achieve the desired attitude changes. Electric servo-actuators receive control signals from the pilot through an RF receiver in the form of a position reference signal. The key difference between the two systems is that the hydro-mechanical actuator receives a physical input through the aircraft control linkages, whilst the electric servo-actuator requires a controller to decode the position reference signal and drive the servo-actuator motor to achieve and maintain the desired position. The ability of the electric servo-actuator to accurately acquire and maintain the desired angle under load is a key performance factor for the helicopter control input response.

Previous work in this area has been focused on the system identification, design and optimisation of servo-actuator controllers (Wada et al. [2009]). As the servo-actuator is a commercially available product, the internal structure is unknown and the performance of the device cannot be altered or tuned. For the purpose of helicopter actuators, the structure of the controller is not as important as the overall system dynamics. The work of the controller is considered internal to the servo-actuator system and

not easily measurable; however its ability to track and maintain the desired output angle is directly measurable. The overall system performance, both free and under load is the focus of this paper.

The inclusion of servo-actuator dynamics within the helicopter mathematical models is considered standard practice. An initial approach was to include basic actuator dynamics through a generic transfer function (McLean. [1990]). This was further expanded to include separate system identification activities to capture the servo-actuator dynamics. This activity is usually conducted off aircraft, either free or with a fixed load. It has been noted that investigating the behaviour of the servo-actuator under actual flight loading may be beneficial to the overall model performance (Mettler. [2003]).

This activity has been undertaken in support of research focusing on the performance of advanced control methodologies for the implementation of helicopter based automatic flight control systems. An ALIGN T-Rex 700E scaled RC helicopter has been modified and instrumented for the purpose of airborne control performance analysis. The servo-actuator identification results from this experiment will be used for the development of a non-linear model of the T-Rex 700E dynamics.

The outline of this paper is as follows. Section 2 will discuss aspects of the helicopter actuator, linkage and main rotor system required to understand the design of the identification experiments. Section 3 will describe the identification methodology used to obtain the Finite Step Response (FSR) model of the servo system using Frequency Sampling Filters (FSF) where the high frequency components of the FSF model is neglected. Section 4 will

describe the methodology for the bench top and flight load experiments and present the relevant results. Section 5 concludes the paper.

2. HELICOPTER ROTOR SYSTEM

The servo-actuator performance experiment will be expanded beyond the standard free or fixed load bench test to include an aircraft load response component. The helicopter main rotor system presents an asymmetric load condition, where an increase in blade pitch will encounter greater resistance than farthing the blades. It is this unique operating environment which is of interest when developing the non-linear model. A brief introduction to the helicopter rotor and actuator linkage system is provided in the following sections to enable a better understanding of the experiments design.

2.1 The Main Rotor System

Helicopter flight is achieved by augmenting the thrust produced by the main rotor system. Vertical motion is achieved by altering the pitch of the rotor blades, thus increasing the angle of attack of the blades collectively as they rotate. Collective input controls the magnitude of the thrust. In order to manoeuvre the helicopter, the direction of the thrust needs to be altered. The most common way of achieving this is by manipulating the blade pitch periodically (or cyclically) during each full rotation, generating an oscillatory flapping motion which in turn tilts the rotor disk. The flapping motion allows the blade thrust vector to be tilted away from vertical, resulting in translation of the helicopter in free space. Fig. 1 shows the main rotor blade control scheme. The book by Stepniewski & Keys. [1984] provides a detailed description of the main rotor system.

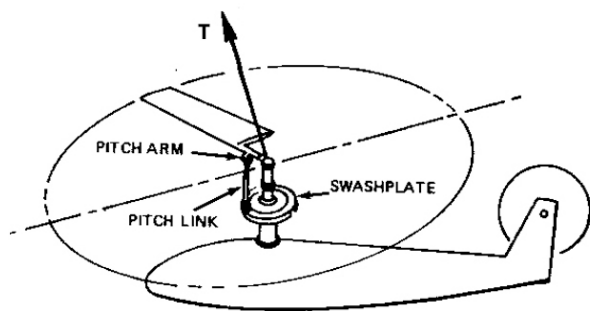


Fig. 1. Helicopter main rotor control scheme (Stepniewski & Keys. [1984])

2.2 Actuator and Linkage System

The actuator and linkage system represents the first stage of a helicopter non-linear model. Unlike conventional fixed-wing aircraft, the helicopters main rotor blades are responsible for the production of lift as well as the implementation of flight control changes. Since the helicopter is the only aircraft which has its wings travelling faster than the fuselage, implementing control inputs is significantly more complicated.

The manipulation of blade pitch takes place as the rotor blades are moving at up to 2000 RPM. At this speed, any change in pitch will require significant force to overcome the resulting aerodynamic forces. A relatively simple device known as a swash plate transfers the control inputs from the stationary fuselage to the rotating rotor disk. Control inputs produced by the servo-actuators are transferred to the swash-plate by control linkages, producing lateral and longitudinal tilting of the swash-plate. The servo-actuators, control linkages and swash-plate represent the first stage of the helicopter non-linear model. The actuator stage input is the servo position reference signal and the output is the lateral and longitudinal swash-plate tilt. Fig. 2 shows the first stage control linkage arrangement for the ALIGN T-Rex 700E RC helicopter.

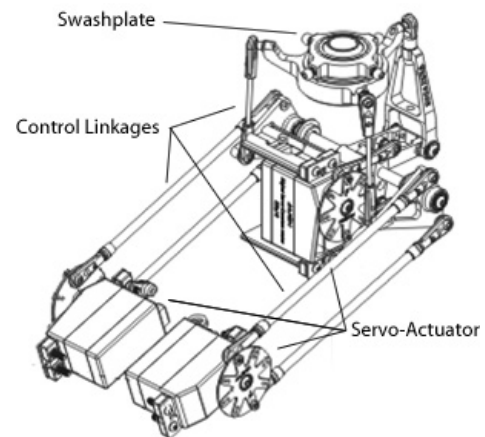


Fig. 2. T-Rex 700E control linkages with 3 servos in a 120° Collective Cyclic Pitch Mixing (CCPM) arrangement

The electric servo-actuator is essentially a simple position control system. It receives a position reference signal in the form of a Pulse Width Modulation (PWM) signal and drives the internal electric motor to achieve and maintain the desired position. Position feedback is provided to the controller through a potentiometer, mechanically coupled within the servo-actuator output gearing system. Fig. 3 shows a block diagram of an RC servo-actuator system.

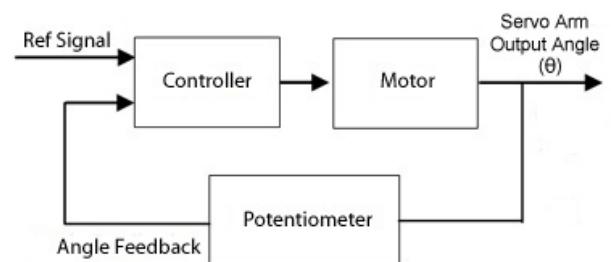


Fig. 3. RC servo-actuator system block diagram

3. CONTINUOUS-TIME SYSTEM IDENTIFICATION USING FSF

A system identification approach is proposed by Gawthrop & Wang. [2005] through which a Finite Impulse Response (FIR) or Finite Step Response (FSR) model can be estimated by applying a FSF. The FSF model structure is advantageous as it is a non-parametric representation

of the system dynamics via frequency decomposition, in which the high frequency components, both dynamics and noise are suitably neglected. The book by Wang & Cluett. [2000] provides a comprehensive outline of this approach.

Assume that the continuous time system is stable with transfer function $G_c(s)$. The system is sampled uniformly with an interval Δt , and the system has a settling time T_s such that when $t \geq T_s$, the impulse response $h(t) \approx 0$. The corresponding discrete parameter to T_s is $N = \frac{T_s}{\Delta t}$. The discrete transfer function of the system can be represented in terms of the frequency response coefficients via the FSFs expression Wang & Cluett. [2000]:

$$G(z) = \sum_{l=-\frac{n-1}{2}}^{\frac{n-1}{2}} G(e^{j\Omega}) H^l(z) \quad (1)$$

where n is an odd number to represent the number of frequencies included in the FSFs model; Ω is the discrete fundamental sampling frequency defined by $\Omega = \frac{2\pi}{N}$ radians. This form allows us to ignore the high frequency content of the signal. The l th frequency sampling filter is given as

$$H^l(z) = \frac{1}{N} \frac{1 - z^{-N}}{1 - e^{j\Omega} z^{-1}} \\ = \frac{1}{N} (1 + e^{j\Omega} z^{-1} + \dots + e^{j(N-1)\Omega} z^{-(N-1)})$$

At $z = e^{j\Omega}$, $H^l(z) = 1$. Equation (1) can also be written in terms of real and imaginary parts of the discrete frequency response $G(e^{j\Omega})$ (Bitmead & Anderson. [1981]) as

$$G(z) = \frac{1}{N} \frac{1 - z^{-N}}{1 - z^{-1}} G(e^{j0}) \\ + \sum_{l=1}^{\frac{n-1}{2}} [Re(G(e^{j\Omega}) F_R^l(z)) \\ + Im(G(e^{j\Omega}) F_I^l(z))] \quad (2)$$

where $F_R^l(z)$ and $F_I^l(z)$ are the l th second order filters given by

$$F_R^l(z) = \frac{1}{N} \frac{2(1 - \cos(l\Omega)z^{-1})(1 - z^{-N})}{1 - 2\cos(l\Omega)z^{-1} + z^{-2}} \\ F_I^l(z) = \frac{1}{N} \frac{2\sin(l\Omega)z^{-1}(1 - z^{-N})}{1 - 2\cos(l\Omega)z^{-1} + z^{-2}}$$

The FSFs model can be regarded as a hybrid structure between a continuous time system and a discrete time system when the sampling interval Δt is sufficiently small. For the continuous time frequency $\omega \leq \frac{\pi}{\Delta t}$, the continuous time frequency response $G_c(j\omega) \approx G(e^{j\omega\Delta t})$. Therefore, the coefficients of the discrete model are corresponding to continuous time frequency response at $\omega = 0, \frac{2\pi}{T_s}, \frac{4\pi}{T_s}, \dots, \frac{\pi}{\Delta t}$.

Suppose that $u(k)$ is the process input, $y(k)$ is the process output and $v(k)$ is the disturbance signal. The output $y(k)$ can be expressed in a linear regression form by defining the parameter vector and the regressor vector as

$$\theta = \begin{bmatrix} G(e^{j0}) \\ Re(G(e^{j\Omega})) \\ Im(G(e^{j\Omega})) \\ \vdots \\ Re(G(e^{j\Omega\frac{n-1}{2}})) \\ Im(G(e^{j\Omega\frac{n-1}{2}})) \end{bmatrix} \phi(k) = \begin{bmatrix} f(k)^0 \\ f(k)_R^1 \\ f(k)_I^1 \\ \vdots \\ f(k)_R^{\frac{n-1}{2}} \\ f(k)_I^{\frac{n-1}{2}} \end{bmatrix}$$

where

$$f(k)^0 = \frac{1}{N} \frac{1 - z^{-N}}{1 - z^{-1}} u(k)$$

$$f(k)_R^l = F_R^l(z)u(k); f(k)_I^l = F_I^l(z)u(k)$$

for $l = 1, 2, \dots, \frac{n-1}{2}$. This allows us to write the linear regression with correlated residuals as

$$y(k) = \phi(k)^T \theta + v(k) \\ v(k) = \frac{\epsilon(k)}{D(z)} \quad (3)$$

where $\epsilon(k)$ is a white noise sequence with zero mean and standard deviation σ . Given a set of sampled finite amount of data

$$\{y(1), y(2), y(3), \dots, y(M)\} \\ \{u(1), u(2), u(3), \dots, u(M)\}$$

we can obtain an estimate of the FSF model and an estimate of the noise model $\frac{1}{D(z)}$ using the generalised Least Squares method (Clarke. [1967], Soderstrom. [2005]). More specifically, in the core estimation algorithm, we let

$$y_D(k) = \hat{D}(z)y(k); \phi_D(k) = \hat{D}(z)\phi(k)$$

The estimation of $\hat{\theta}$ is obtained by minimising the quadratic performance index

$$J = \sum_{k=1}^M [y_D(k) - \phi_D(k)\theta]^2 \\ = \theta^T \sum_{k=1}^M [\phi_D(k)\phi_D(k)^T] \theta \\ - 2\theta^T \sum_{k=1}^M [\phi_D(k)y_D(k)] + cons \quad (4)$$

$\hat{D}(z)$ is estimated from the error sequence $e(k) = y(k) - \phi(k)^T \hat{\theta}$, $k = 1, 2, 3, \dots, M$. The generalised Least Squares method is based on an iterative procedure and the iteration stops after the estimated parameters converge.

In order to obtain the estimated step response from the estimated frequency parameter vector θ , it can be easily verified (Wang & Cluett. [2000]) that the step response of the system at the sample m is in a linear relation to the frequency parameter vector θ via

$$\hat{g}_m = Q(m)^T \hat{\theta} \quad (5)$$

where

$$Q(m) = \begin{bmatrix} \frac{m+1}{N} \\ 2\text{Re}(S(1, m)) \\ 2\text{Im}(S(1, m)) \\ \vdots \\ 2\text{Re}(S(\frac{n-1}{2}, m)) \\ 2\text{Im}(S(\frac{n-1}{2}, m)) \end{bmatrix}$$

$$S(l, m) = \frac{1}{N} \frac{1 - e^{j\Omega(m+1)}}{1 - e^{j\Omega}}, \quad l = 1, 2, \dots, \frac{n-1}{2}.$$

4. IDENTIFICATION EXPERIMENT

The identification experiments were performed on the ALIGN DS610 servo-actuator, which has a 100 degree range of motion. The measurements were taken using a Honeywell RTY Series hall-effect rotary position sensor. This sensor has a 120 degrees sensing range and provides a stable and calibrated analogue linear output between 0.5-4.5 volts.

The PWM servo-actuator position reference signal was generated using a 32-bit STMicroelectronics CORTEX-M3 microcontroller. The reference signal consisted of a PWM pulse train with a period of 20 ms. The servo position could be controlled over the full operating range by adjusting the duty cycle within the range of 1-2 ms. The input signal utilised during the identification experiment is shown in Fig. 4. The signal traverses the servo over a ± 5 degree range, maintaining each position initially for 800 ms, decaying each cycle by 100 ms. This reference signal contains sufficient frequency content for the FSF identification algorithm.

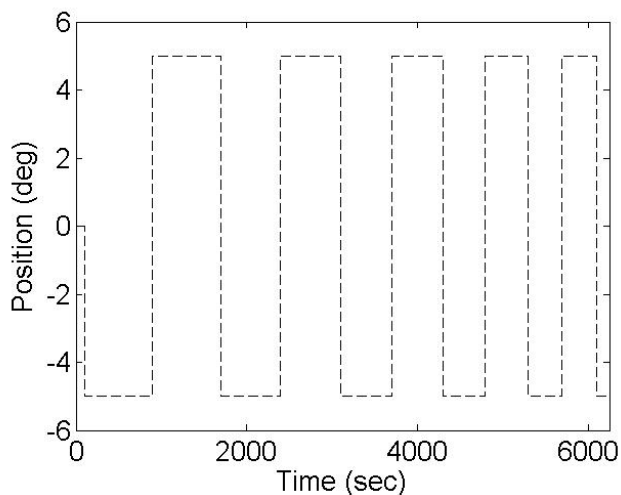


Fig. 4. Position reference signal ($\pm 5^\circ$ displacement)

Two independent identification experiments were conducted. The first experiment consisted of a bench-top position sweep with no load on the sensor. The second involved a position sweep with the sensor mounted to the helicopter main rotor system.

4.1 Bench-top Experiment

The sensor was mounted onto the servo-actuator using a custom mounting bracket and sensor retaining plate. The servo-actuator output shaft was coupled to the sensor via a rigid link, and the entire assembly was supported using a fixing bracket attached to the workbench. The data was recorded using a 2 Gsa/sec Digital Storage Oscilloscope at a sampling rate of 2 ms. The servo-actuator FSR model was estimated using the FSF based upon the recorded input and output data. Fig. 5 and 6 show the step response and frequency response estimates respectively. A comparison between the servo-actuator and the model output is shown in Fig. 7. Overall, the model was able to accurately reproduce the dynamic response of the servo-actuator system.

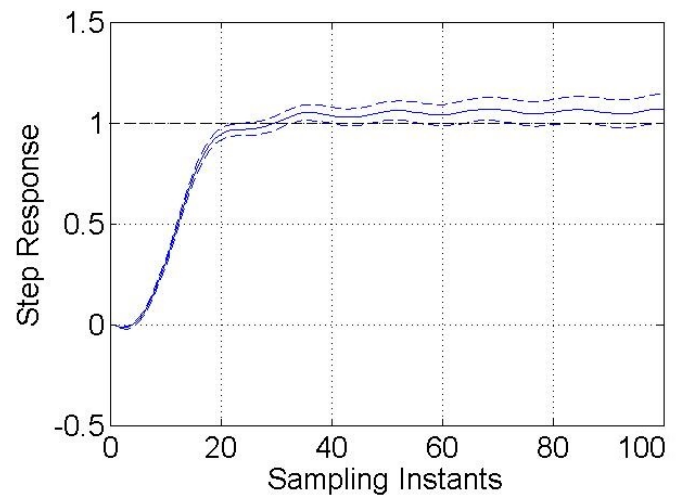


Fig. 5. Bench test FSF step response estimate (solid: FSF, dashed: 99% confidence bounds)

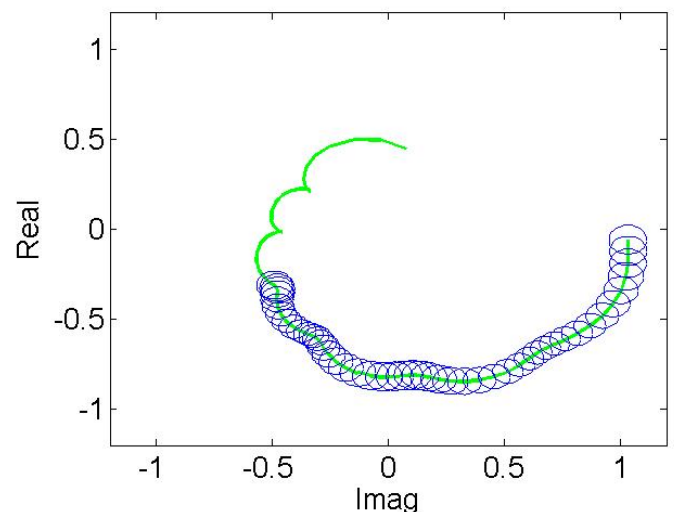


Fig. 6. Bench test FSF frequency response estimate

4.2 Flight Load Experiment

For the aircraft load test, the servo was installed onto the aircraft as part of the CCPM main rotor system.

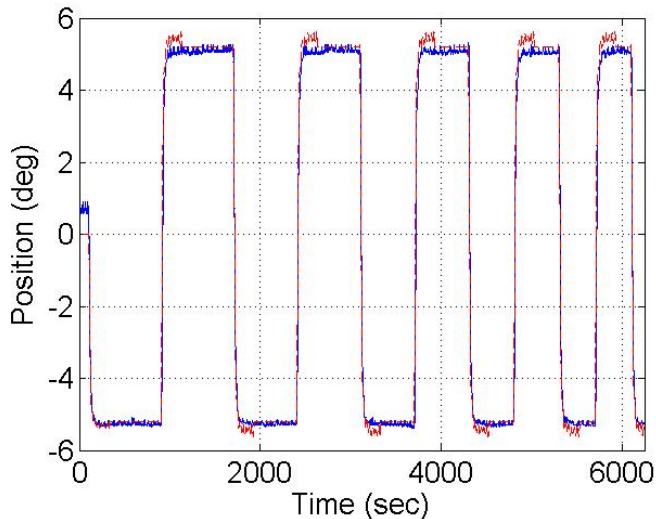


Fig. 7. Bench test model validation (red: Model output, blue: Measurement data)

The T-Rex 700E was modified to incorporate a 4 blade main and tail rotor system instead of the standard 2 blade arrangement. This was done to eliminate the mechanical stabiliser bar, which better reflects modern helicopters. The sensor was coupled with the servo-actuator in exactly the same manner, however the assembly was now secured to the helicopter fuselage. For general flight, the recommended blade pitch range is 0-12 degrees and a rotor speed of 1400 RPM. The experiment was designed to replicate a hover condition. It was identified that 6 degrees of collective pitch was required for the aircraft to achieve lift-off and remain airborne. A ± 5 degree servo displacement, which induced a 4 degree change in blade pitch was selected to ensure the maximum blade pitch limit of 12 degrees was not exceeded. The helicopter was tethered to a test rig, allowing ± 10 degrees of rotation about the lateral axis in order to avoid damage to the rotor system as the thrust is angled away from the vertical position. The position input signal and sampling rate remain unchanged from the bench test experiment. The results are shown in Fig. 8.

4.3 Experiment Comparison

A comparison between the bench test model and aircraft test data is shown in Fig. 9. The data indicates that the model overestimated the actual in flight servo-actuator position by 22%. This result was expected as the model does not take into account the asymmetric load imposed by the main rotor as the blade pitch is increased. In this case, the servo-actuator is saturated and the desired +5 degree position (+10 degree overall blade pitch) is never achieved.

The FSF analysis procedure was performed on the aircraft test data. The estimated step response, frequency response and model output are shown in Fig. 10, Fig. 11 and Fig. 12 respectively.

The estimated step response for both models is shown in Fig. 10. The results indicate that the bench and aircraft test models exhibit significantly different dynamics. The

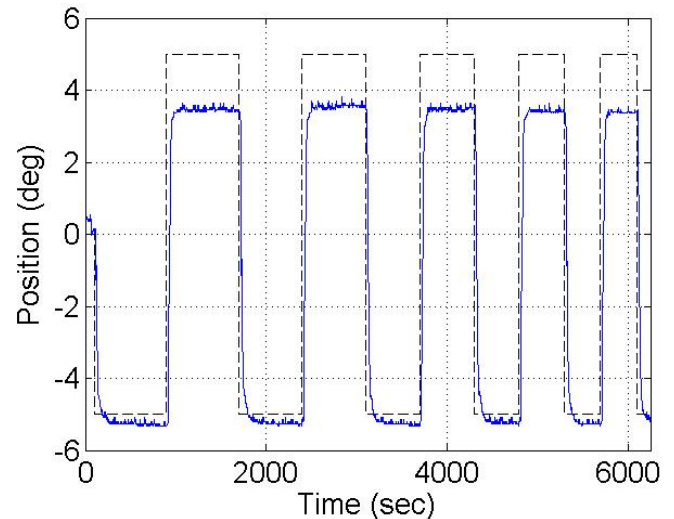


Fig. 8. Aircraft test measurement data (black: Input signal, blue: Aircraft measurement data)

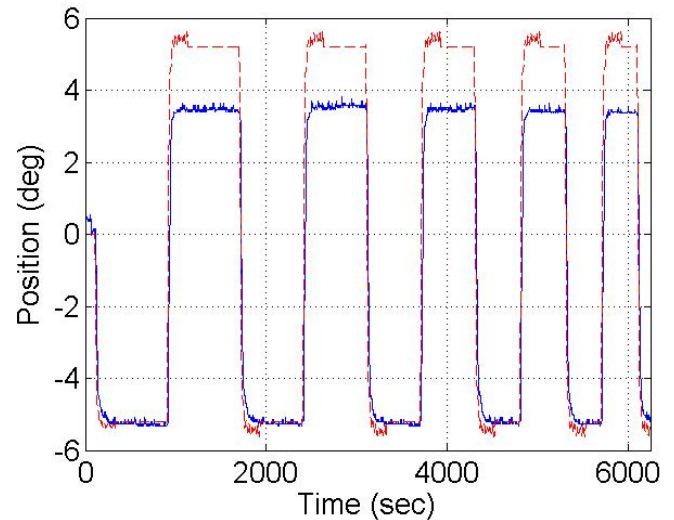


Fig. 9. Comparison of Bench test FSR model and Aircraft test data (blue: Aircraft data, red: Bench test model)

bench test model achieves steady state in approximately 60 sampling intervals. The aircraft model step response indicates a slower initial response, however as the asymmetric load increases, the system exhibits an oscillatory behaviour and continues to push towards the set-point. The estimated frequency response shown in Fig. 11 can be compared to the bench test frequency response in Fig. 6.

A comparison of the position reference signal and the estimated bench and aircraft test models is shown in Fig. 12. The data shows that the bench test model overshoots the set-point by approximately 0.2 degrees and exhibits transient oscillation. The aircraft test response exhibits an initial peak and eventually undershoots the set-point by approximately 1.2 degrees.

The comparable difference in system dynamics and final position for both conditions indicates that the servo-actuator system exhibits significantly varying performance

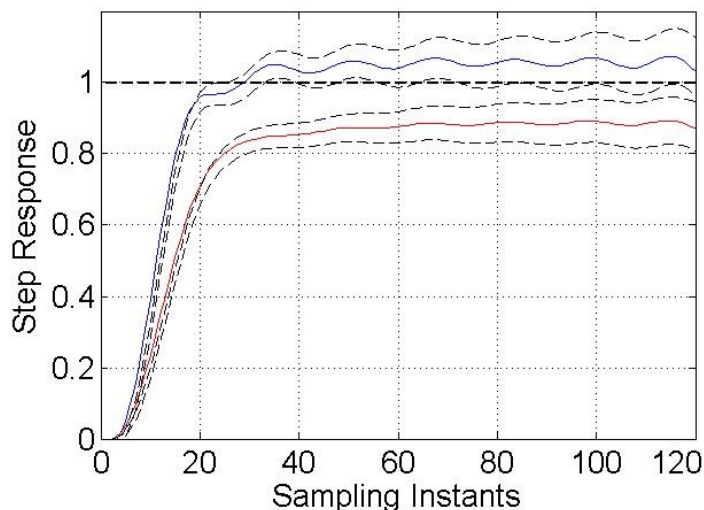


Fig. 10. Aircraft test FSF step response comparison (blue: Bench test step response estimate, red: Aircraft test step response estimate, dashed: 99% confidence bounds)

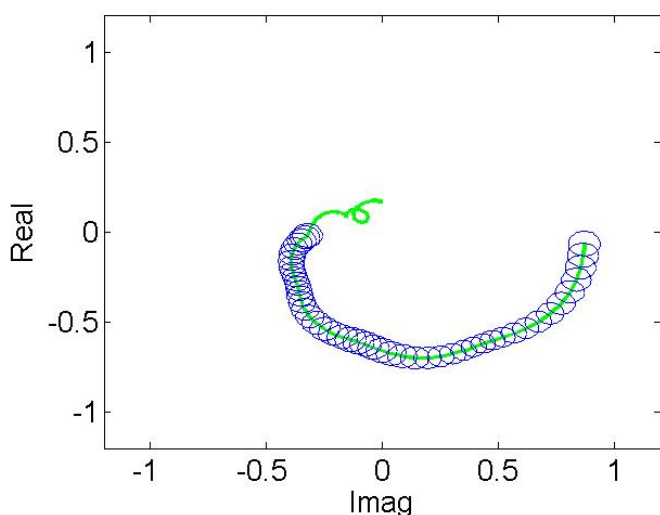


Fig. 11. Aircraft test FSF frequency response estimate when subjected to a load condition. For control system design, the aircraft test model must be considered as the system will be continuously exposed to an asymmetric and variable load condition as the helicopter manoeuvres in free space. The overall conservative undershoot is a better representation of the servo position, and subsequently the swash-plate tilt for the actuator and control linkage stage of the helicopter non-linear model.

5. CONCLUSION

In this paper, models for an electric RC servo-actuator were estimated using the FSF approach under a standard bench test and aircraft load condition. The intent of this work was to validate the performance of the bench test model under realistic flight conditions. The results indicate that the load imposed on the servo-actuator has a significant enough effect to invalidate the bench test model

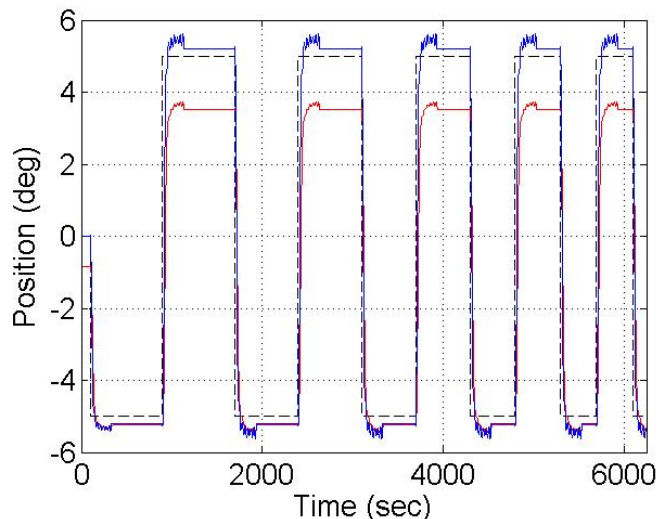


Fig. 12. FSF model comparison (black: Position reference signal, blue: Bench test model, red: Aircraft test model)

during general flight. The maximum blade pitch predicted by the model is never achieved, hence the helicopter response and aerodynamic forces will be over-predicted by the non-linear model. Since the servo-actuators do not provide external position feedback, and measuring the blade pitch of the helicopter in flight is not possible, identifying this under performance will be difficult.

A possible solution may be to select a servo-actuator that has a higher torque rating which is able to function effectively under the T-Rex 700E load conditions.

REFERENCES

- Bitmead, R. R., and B. D. O. Anderson *Adaptive frequency sampling filters*. IEEE Trans. on Circuits and Systems, **28**, 524-533, 1981.
- Clark, D. W. *Generalized least squares estimation of parameters of a dynamic model*. First IFAC Symposium on Identification and Automatic Control Systems, Prague, 1967.
- Gawthrop, Peter, and Liuping Wang. *Data Compression for Estimation of the Physical Parameters of Stable and Unstable Linear Systems*. Automatics, **41**(8), 1313-1321, 2005.
- McLean, Donald. *Automatic Flight Control Systems*. New York, London, Prentice Hall, 1990.
- Mettler, Bernard. *Identification, Modelling and Characteristics of Miniature Rotorcraft*. Boston, Kluwer Academic Publishers, 2003.
- Soderstrom, T. *Convergence properties of the generalized east square method*. Automatica, **10**, 617-626, 1974.
- Stepniowski, W. Z., and C.N. Keys & Keys *Rotary-Wing Aerodynamics*. New York, Dover Publications, 1984.
- Wada, Takashi, M. Ishikawa, R. Kitayoshi, I. Maruta, and T. Sugie *Practical Modeling and System Identification of R/C Servo Motors*. Proceedings of the IEEE Multi-Conference on Systems and Control, 1378-1383, 2009.
- Wang, Liuping, and William R. Cluett. *From plant data to process control*. London, New York, Taylor & Francis, 2000.